Journal of ELECTRICAL ENGINEERING, VOL 70 (2019), NO2, 171–175

sciendo

COMMUNICATIONS

Formation of nanocrystalline alloys after Cu ions implantation into amorphous precursor

Jozef Sitek, Dominika Holková, Július Dekan, Milan Pavúk, Patrik Novák*

Amorphous precursors of A: $(Fe_{64}Co_{21}B_{15})_{95}P_4Cu_1$ and B: $(Fe_{64}Co_{21}B_{15})_{96}P_4$ alloys were used. Nanocrystalline structure was created by heat treatment. Samples were studied by Mössbauer spectroscopy, XRD and AFM. Cu ions of dose 10^{16} at/cm^2 were implanted into the amorphous B. According to simulated program we estimated that Cu ions created surface layer with a thickness of a few micrometres. Changes in bulk structure were not observed at parameters of Mössbauer spectra after implantation. After heat treatment the implanted sample was nearly identical with the nanocrystalline sample of A. Implantation had an influence on the volumetric fraction of the constituent phases and on their magnetic microstructure. Implantation of Cu ions in amorphous precursor containing Cu as A caused after heat treatment in nanocrystalline state increasing of nanocrystalline component. This technology of preparation of nanocrystalline alloys indicate that implantation of ions into an amorphous precursor has an influence on the final structure and properties of nanocrystalline alloy.

K e y w o r d s: amorphous alloys, nanocrystalline alloys, radiation damage, Mössbauer spectroscopy

1 Introduction

In the recent years, nanocrystalline alloys have become attractive for many applications. The most prominent FINEMET, NANOPERM and HITPERM-type alloys have been frequently investigated because they exhibit excellent soft magnetic properties. Recently soft magnetic alloys NANOMET were developed as FeSiBCu and FeSiBPCu alloys [1]. It was also found that substitution of Co for Fe improved the soft magnetic properties and thermal stability of the nanocrystalline alloys [2].

The crystallization process of the amorphous precursor is known to be controlled by thermal annealing. It has been already shown that nanocrystalline structure could be more or less realized or affected by external factors [3, 4] such a neutron and electron irradiation [5, 6].

Changes in the orientation of the average magnetic moment were observed by Mössbauer spectroscopy in neutron irradiated metallic glasses and nanocrystals [7]. The particle bombardment produces defects that may cause a realignment of magnetic domains implying a reorientation of the magnetic moments. Changes in the local neighbourhoods of the atoms affect the average hyperfine magnetic field as well as the shape of the hyperfine field distributions. In the case of nanocrystalline alloys, which consist of crystalline nanograins embedded in an amorphous intergranular matrix, irradiation by neutrons will lead to redistribution of atoms in the amorphous matrix, disturbance of regular atomic ordering of the crystal lattice and atom exchange between the amorphous and crystalline component.

Effect of electron irradiation on the crystallization of NANOMET alloys also was examined [8]. In this case Fe nanocrystals changes were observed in the irradiated amorphous matrix. Electron knock-out effect assists atomic diffusion and accelerated the crystallization of amorphous precursor. By electron irradiation rearrangement of large quantity of defects are produced, interstitials and vacancies are continuously moved. Then the final structure after thermal annealing is different from the structure without irradiation.

Nanocrystalline $(Fe_{64}Co_{21}B_{15})_{95}P_4Cu_1$ and $(Fe_{64}Co_{21}B_{15})_{96}P_4$ alloys were also modified after electron irradiation of their precursors of the doses up to 4 MGy, which was indicated from phase analysis of irradiated and non-irradiated alloys [9].

Our work is focused on the structural modification of selected nanocrystalline alloys after Cu implantation in amorphous precursors. It was shown that such an implantation has an influence at the ratio of amorphous and crystalline components of final nanocrystalline alloy.

2 Experimental details

The samples for Mössbauer experiment were studied in form of ribbon produced by planar flow casting of the melt at the Physical Institute SAS in Bratislava. Implantation of Cu ions was performed at Faculty of Materials Science and Technology in Trnava with fluence 10^{16} ions/cm^2 and energy of 2 MeV.

Annealing at 400 °C was performed in GLS-1800X-KS60 tube furnace. The trend of achieving of the tem-

* Institute of Nuclear and Physical Engineering, Slovak University of Technology, Ilkovičova 3, Bratislava, Slovakia, jozef.sitek@stuba.sk, milan.pavuk@stuba.sk

DOI: 10.2478/jee-2019–0025, Print (till 2015) ISSN 1335-3632, On-line ISSN 1339-309X

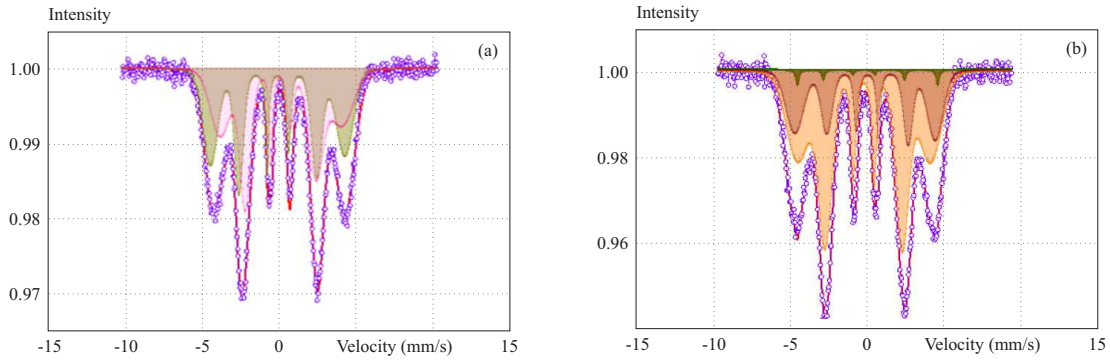

Fig. 1. (a) – Mössbauer spectrum of $(Fe_{64}Co_{21}B_{15})_{96}P_4$ alloy, (b) – Mössbauer spectrum of $(Fe_{64}Co_{21}B_{15})_{96}P_4$ alloy after Cu implantation; the dark green sextet represents traces of a crystalline component.

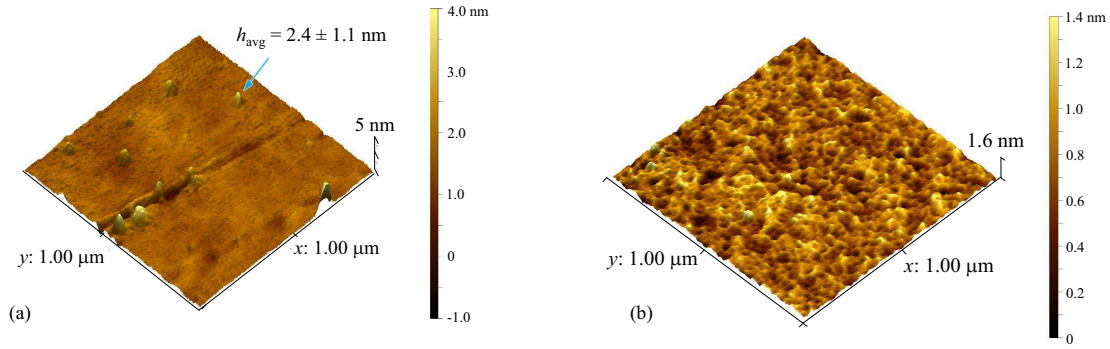

Fig. 2. 3D AFM image showing surface of shiny side of: (a) – non-implanted, and (b) – Cu implanted as-quenched $(Fe_{64}Co_{21}B_{15})_{96}P_4$ alloy. The h_{avg} parameter denotes an average height of protrusions at the scanned surface with given standard deviation.

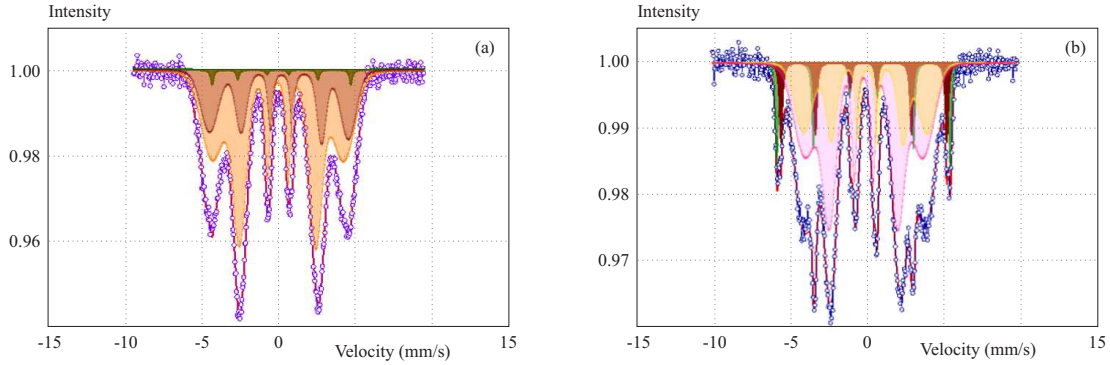

Fig. 3. (a) – non-implanted nanocrystalline $(Fe_{64}Co_{21}B_{15})_{96}P_4$, (b) – Implanted nanocrystalline $(Fe_{64}Co_{21}B_{15})_{96}P_4$

perature was performed according to the allowed heating rates (5/min). At 200 °C there was settling time for 120 minutes. This was mainly because of the stabilization of vacuum parameters at level of $10^{-3}-10^{-4}$ Pa. The temperature increased after stabilization within 40 min to 400 °C . The specimens were annealed for 30 min and afterwards were gradually cooled down (max. 5 °C /min) to room temperature. Thickness of the samples was a 25 microns.

The Mössbauer spectra were measured at room temperature using a Wissel Mössbauer spectrometer with the Co^{57} (Rh) source in transmission geometry. Spectrometer was calibrated using a standard foil of α-Fe at room temperature. The hyperfine parameters of the spectra including relative component area (A_{rel}), isomer shift (IS), quadrupole splitting (QS), as well as internal hyperfine magnetic field (B_{hf}). Spectra were evaluated by CONFIT program [10] allowing simultaneous treatment of crystalline components and residual amorphous phases using individual lines and distributions of hyperfine parameters. The accuracy in their determination is about 2 % for the relative area, 0.04 mm/s for the isomer shift and quadrupole splitting and about 0.5 T for the hyperfine magnetic field.

Surface morphology of both ribbons before and after implantation was observed using Dimension Edge^{TM} (Veeco, USA) Atomic Force Microscope (AFM). The microscope is placed on a pneumatic antivibration table and during measurements it was shielded with acoustic cover. All 3D-AFM images have the z-scale stretched in a way that 1 nm on the axis has always the same length.

Table 1. Spectral parameters of non-implanted and implanted $(Fe_{64}Co_{21}B_{15})_{96}P_4$

	Component	Amorphous			Nanocrystalline		
		A_{23} (-)	B (T)	A (%)	A_{23} (-)	B (T)	A (%)
Non-implanted	Amorphous high	2.47	27.9	49	2.42	28.6	34
	Amorphous low	3.76	25.3	51	3.62	26.5	64
	Crystalline	-	-	-	2.36	31.44	2
Implanted	Amorphous high	2.20	27.9	32	2.16	26.5	28
	Amorphous low	3.55	26.2	65	3.21	25.2	54
	Crystalline high	2.00	30.8	3	2.44	37.0	10
	Crystalline low	-	-	-	2.71	35.5	8

X-ray diffraction (XRD) patterns were recorded in standard geometry using diffractometer D8 Advance (Bruker, USA) and Co K_α radiation.

3 Results and discussion

Mössbauer spectra of all samples were evaluated preferably using a model comprising two distributions of sextets representing the amorphous rest and one or two sextets describing the crystalline phase. Mean value of distribution of internal magnetic field of amorphous rest corresponds to superposition of high and low field component. Spectra of the $(Fe_{64}Co_{21}B_{15})_{96}P_4$ amorphous alloy before and after implantation of Cu ions are shown on Fig. 1(a) and Fig. 1(b), respectively. After implantation, changes in the orientation of the net magnetic moment, in the value of the average hyperfine magnetic field of the amorphous and crystalline components and of their volumetric fraction took place. Orientation of the net magnetic moment is reflected by the ratio of the second- and fifth-line intensities of a Mössbauer spectrum (A_{23}). This parameter achieves its maximum value if the direction of the net magnetic moment lay in sample plane and its minimum value, when oriented perpendicular to the sample plane.

After Cu implantation of amorphous $(Fe_{64}Co_{21}B_{15})_{96}P_4$ alloy we observed traces of crystalline component till 2 % which is near the error and decrease of A_{23} parameter what indicates that net magnetic moment turns out of the ribbon plane. Mössbauer parameters of the investigated alloys before and after Cu implantation are given in Tab. 1.

Surface of the $(Fe_{64}Co_{21}B_{15})_{96}P_4$ alloy was analysed by AFM method. Most important was shiny side because from this side Cu implantation was performed. AFM records are shown in Fig. 2(a) and Fig. 2(b), respectively. The pictures of non-implanted and implanted samples show that after implantation changes in the surface morphology occurred. This is an evidence that Cu ions after implantation were concentrated on the surface.

To obtain the Cu implantation profile, SRIM simulation software was used [11]. According to calculation the depth of implanted Cu was approximately 1.4 μm into the sample with thickness of 25 μm.

Mössbauer spectra after thermal treatment are shown in Fig. 3(a) and 3(b), respectively. Parameters of the investigated alloys before and after Cu implantation are given in Tab.1.

After thermal treatment of non-implanted sample, the $(Fe_{64}Co_{21}B_{15})_{96}P_4$ alloy did not transform into nanocrystalline state in the whole volume and we observed only traces of the crystalline component in the frame of error. Decrease of A_{23} parameter indicates that the net magnetic moment turns out of the ribbon plane. We also observed changes in relative amount of high and low field magnetic component.

Small addition of Cu due to implantation caused transition into fully nanocrystalline state only after thermal treatment. Crystalline component was identified according to value of internal magnetic field as Fe-Co alloy.

Another sample for the analysis was $(Fe_{64}Co_{21}B_{15})_{95}P_4Cu_1$ alloy containing Cu and this one was compared with the former without Cu. Mössbauer spectra of non-implanted and implanted amorphous precursor are nearly identical with the Mössbauer spectra of amorphous $(Fe_{64}Co_{21}B_{15})_{96}P_4$ alloy shown in Fig. 1. Mössbauer parameters are given in Tab. 2. Analysis by AFM method of shiny side showed surface changes after Cu implanted in amorphous sample as in former case and it is shown in Fig. 4.

Mössbauer spectra after thermal treatment are presented in Fig. 5. After thermal treatment crystalline component Fe-Co was identified in amorphous rest. Non-implanted annealed sample contained 16 % of crystalline fraction and the implanted one 28 %. Changes in the magnetic structure observed via increased A_{23} parameter indicate that the direction of net magnetic moment turn into the ribbon plane. It is contrast to $(Fe_{64}Co_{21}B_{15})_{96}P_4$ alloy where the net magnetic moment turns out of the ribbon plane.

Nanocrystalline samples were also analysed by XRD. Diffractograms of non-implanted and implanted alloys are shown in Fig. 6. From XRD analysis was found that non-implanted sample contains 16 % of crystalline component and implanted one 27 % which agrees with the results achieved from Mössbauer spectroscopy.

Table 2. Spectral parameters of non-implanted and implanted $(Fe_{64}Co_{21}B_{15})_{95}P_4Cu_1$

	Component	Amorphous			Nanocrystalline		
		A_{23} (-)	B (T)	A (%)	A_{23} (-)	B (T)	A (%)
Non-implanted	Amorphous high	2.14	28.0	36	2.80	25.9	40
	Amorphous low	3.71	26.0	64	2.84	25.5	44
	Crystalline high	-	-	-	2.70	37.1	8
	Crystalline low	-	-	-	3.39	35.7	8
Implanted	Amorphous high	2.16	28.2	35	2.56	26.8	36
	Amorphous low	3.82	26.2	65	2.55	23.3	36
	Crystalline high	-	-	-	2.77	37.2	14
	Crystalline low	-	-	-	2.28	35.8	14

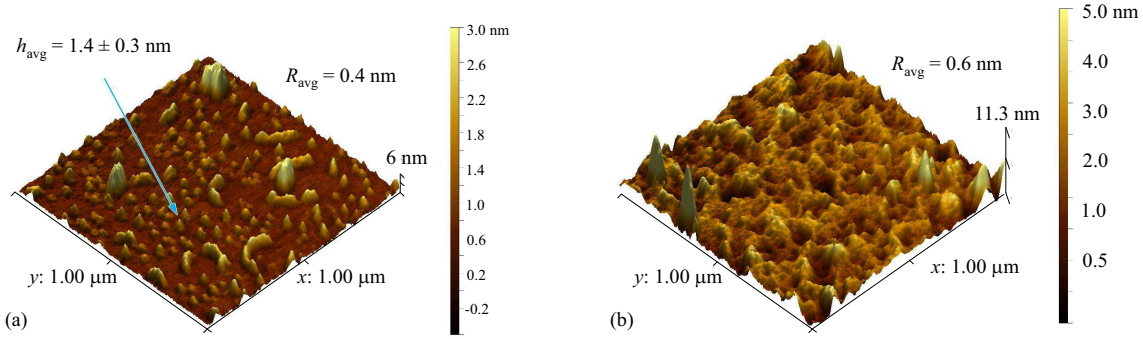

Fig. 4. 3D AFM image showing surface of shiny side of: (a) – non-implanted, and (b) – Cu implanted annealed $(Fe_{64}Co_{21}B_{15})_{95}P_4Cu_1$ alloy. The h_{avg} parameter denotes an average height of protrusions at the scanned surface with given standard deviation.

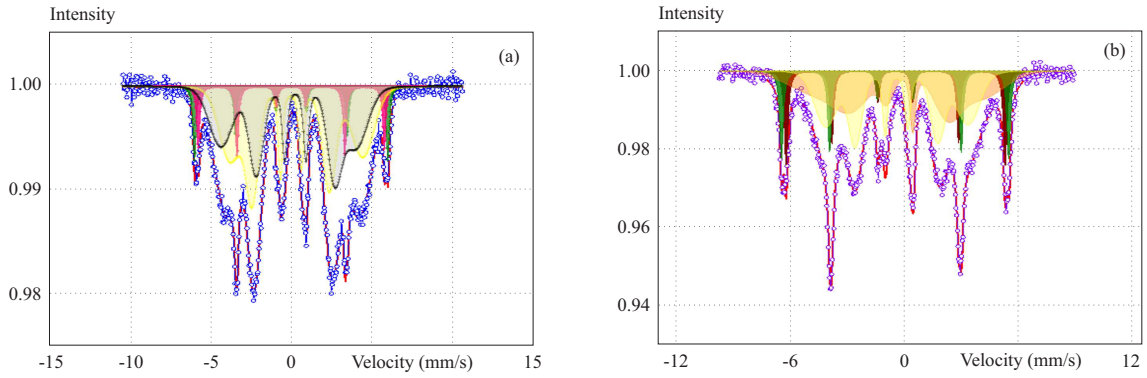

Fig. 5. (a) – Mössbauer spectrum of non-implanted nanocrystalline $(Fe_{64}Co_{21}B_{15})_{95}P_4Cu_1$, (b) – Mössbauer spectrum of implanted nanocrystalline $(Fe_{64}Co_{21}B_{15})_{95}P_4Cu_1$.

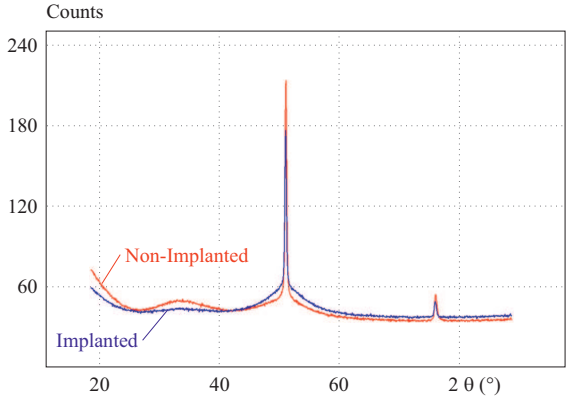

Fig. 6. XRD from non-implanted and implanted nanocrystalline $(Fe_{64}Co_{21}B_{15})_{95}P_4Cu_1$ alloy

Comparison of Cu implanted $(Fe_{64}Co_{21}B_{15})_{96}P_4$ and non-implanted $(Fe_{64}Co_{21}B_{15})_{95}P_4Cu_1$ alloy

Analysis of these both alloys indicate that by increasing the Cu content due to implantation causes increase in amount of crystalline component. We compared average parameters of Mössbauer spectra with Cu implanted alloy and non-implanted alloy containing Cu. Parameters are given in Tab. 3. If we made a comparison of both alloys, we found that their parameters are nearly identical in the frame of error. This make it possible to prepare the alloy with assumed properties by combine technology of implantation and heat treatment.

Table 3. Spectral parameters of non-implanted $(Fe_{64}Co_{21}B_{15})_{95}P_4Cu_1$ and implanted $(Fe_{64}Co_{21}B_{15})_{96}P_4$

Component	Non-implanted nanocrystalline alloy $(Fe_{64}Co_{21}B_{15})_{95}P_4Cu_1$			Implanted nanocrystalline alloy $(Fe_{64}Co_{21}B_{15})_{96}P_4$		
	A_{23} (-)	B (T)	A (%)	A_{23} (-)	B (T)	**A** (%)
Amorphous	2.82	25.7	84	2.69	25.8	82
Crystalline	2.69	36.4	16	2.59	36.3	18

5 Conclusion

It was shown that the implantation of Cu ions into amorphous precursor has an influence on the ratio of amorphous and crystalline components of the final structure of nanocrystalline alloy, as well as at their parameters in amorphous and crystalline state. This give us possibility to prepare final nanocrystalline alloy from precursor after implantation of Cu and thermal treatment according to technological requirement.

Acknowledgements

This work was supported by grant of Ministry of Education, Science, Research and Sport of the Slovak Republic via the projects VEGA 1/0561/17, 1/0477/16 and 1/0182/16.

References

[1] A. Akimo, H. Men, T. Kubota, K. Yubuta, and A. Inoue, *Mat. Trans.* vol. 50, pp. 204–209, 2009.

[2] R. Xiang, S. Zhou, B. Dong, G. Zhang, Z. Li, and Y. Wang Ch Chang, *Progress in Natur. Science: Mat. Inter* vol. 24, pp. 649–654, 2014.

[3] J. Sitek, J. Degmová, and K. Sedlačková, *Journal of Modern Physics* vol. 3, no. 3, pp. 274-277, 2012.

[4] Yong-Qin Chang, Qiang Guo, Jing Zhang, Lin Chen, Yi Long and Fa-Rong Wan *Mater. Sci. Eng.* vol. 7, no. 2, pp. 141-155. 2013.

[5] J. Sitek, D. Holková, J. Dekan, and P. Novák, *AIP Conf. Proc. Mössbauer Spectroscopy in Material Science* vol. 1781, 020003, 2016.

[6] T. Nagase, Y. Umakoshi, and N. Sumida, *Mater. Sci. Eng* vol. A 323, pp. 218-225, 2002.

[7] J. Sitek, J. Dekan, and M. Pavlovič, *Acta Physica Polonica* vol. A 126, no. 1, pp. 84-85, 2014.

[8] K. Shimizu, M. Nishijima, A. Takeuchi, T. Nagasez, H. Yasudaz, and A. Makimo, *J. Jap. Inst. Met.* vol. 78(a), pp. 364-368, 2014.

[9] J. Sitek, D. Holková, J. Dekan, P. Novák, A. Šagátová, and S. Soják, *AIP Conf. Proc. Applied Physics Condensed Matter* 1996, 20043, 2018.

[10] T. Žák and Y. Jirásková, *Surf. Interface Anal.* vol. 38, pp. 710–714, 2006.

[11] D. Holková, "Modification of Amorphous Metallic Alloys Nanocrystals using Radiation", *thesis STU Bratislava*, 2018.

Received 17 December 2018

Jozef Sitek (Prof, Ing, DrSc), born in Zahorská Ves, Slovakia in 1944, graduated from the Faculty of Electrical Engineering, Slovak University of Technology, in 1966. He received his PhD degree in Applied Physics in 1974 and a DrSc degree in Physics of Condensed Matter in 1994. At present at he is Professor for Physical Engineering at the Institute of Nuclear and Physical Engineering, Faculty of Electrical Engineering and Information Technology.

Dominika Holková (Mgr, PhD), born in 1991 in Slovakia, graduated from the Faculty of Natural Science, Comenius University in Bratislava. Her current research is focused on the study amorphous and nanocrystalline alloys under influence of radiation. She finished her doctoral study at the Slovak University of Technology (2018) in the branch of Physical Engineering.

Július Dekan (Ing, PhD), born in 1980 in Bratislava, Slovakia, graduated from the Faculty of Electrical Engineering and Information Technology, Slovak University of Technology in Bratislava in branch Electromaterial Engineering and received the PhD degree in Physical Engineering in 2010. Since 2008 he has worked as a researcher at the Institute of Nuclear and Physical Engineering of Faculty of Electrical Engineering and Information Technology.

Milan Pavúk (Ing, PhD), born in 1980 in Bratislava, Slovakia, graduated from the Faculty of Electrical Engineering and Information Technology, Slovak University of Technology in Bratislava in branch Electromaterial Engineering and received the PhD degree in Physical Engineering in 2010. Since 2008, he has worked as a researcher at the Department of Nuclear Physics and Technology (now Institute of Nuclear and Physical Engineering) at the same university. He specializes in Atomic and Magnetic Force Microscopy (AFM & MFM).

Patrik Novák (Ing, PhD) was born in Ružomberok (Slovakia) in 1987. He is currently a researcher at the Institute of Nuclear and Physical Engineering. He has expertise in studying properties of thin films by X-ray diffraction. His dissertation thesis dealt with an analysis of residual stresses in thin films by grazing incidence X-ray diffraction. His current research is focused on the study of structural information about thin films for water splitting devices and other materials for electronics. He finished his doctoral study at the Slovak University of Technology (2017) in Physical Engineering. He gained professional experience at the Slovak Academy of Sciences and the Center for Nanodiagnostics.